Gabriëlle J. M. Tuijthof
Ph.D.
Department of Orthopedic Surgery,
Orthopedic Research Center Amsterdam,
Academic Medical Centre,
Meibergdreef 9,
1105 AZ Amsterdam, The Netherlands
e-mail: g.j.tuijthof@amc.uva.nl

Paul M. Heeman
B.Sc.
Department of Medical Technological
Development (MTO),
Academic Medical Centre,
Meibergdreef 9,
1105 AZ Amsterdam, The Netherlands
e-mail: p.heeman@amc.uva.nl

C. Niek Van Dijk
Ph.D. M.D.
Professor
e-mail: c.n.vandijk@amc.uva.nl

Leendert Blankevoort
Ph.D.
e-mail: l.blankevoort@amc.uva.nl

Department of Orthopedic Surgery,
Orthopedic Research Center Amsterdam,
Academic Medical Centre,
Meibergdreef 9,
1105 AZ Amsterdam, The Netherlands

Physical Simulation Environment for Arthroscopic Joint Irrigation

Good arthroscopic view is important to perform arthroscopic operations (minimally invasive surgery in joints) safely and fast. To obtain this, the joint is irrigated. However, optimal irrigation settings are not described. To study the complex clinical practice of irrigation, a physical simulation environment was developed that incorporates the main characteristics for performing arthroscopy. Its irrigation capacities were validated with patient data. The physical simulation environment consists of a specially designed knee phantom, all normally used arthroscopic equipment, and registration devices for two video streams, pressures, and flows. The physical embodiment of the knee phantom matches that of human knee joints during arthroscopic operations by the presence of important anatomic structures in sizes comparable to human knee joints, the presence of access portals, and the ability to stress the joint. The hydrostatic and hydrodynamic behavior of the knee phantom was validated with pressure and flow measurements documented during arthroscopic knee operations. Surgeons confirmed that the knee phantom imitated human knee joints sufficiently. The hydrostatic parameters of the knee phantom could be tuned within the range of the human knee joints (restriction: $0.0266-29.3\ N\,s^2/m^8$ versus $0.0143-1.22\times10^{18}\ N\,s^2/m^8$ and capacitance: $6.89\ m^5/N$ versus $7.50\times10^{-9}\ m^5/N$). The hydrodynamic properties of the knee phantom were acceptably comparable to those of the human knee joints. The physical simulation environment enables realistic and conditioned experimental studies to optimize joint irrigation. The foundation has been laid for evaluation of other surgical instruments and of training of surgical skills. [DOI: 10.1115/1.3131729]

Keywords: simulation, arthroscopy, irrigation, design

1 Introduction

In arthroscopic operations (minimally invasive surgery in joints), it is important to keep a clear view on the operation area [1–4]. This is sometimes difficult because disturbances inside the joint, such as blood and debris, can block the view [5]. During arthroscopic procedures, the joint is irrigated with saline to keep the view clear. Additionally, the saline is pressurized to enlarge the available joint space. Irrigation is performed with a pump that leads the saline via an inflow tubing and a sheath into the joint [4]. Two types of pumps are widely used: the classic gravity pump, consisting of a liquid bag placed at a certain height, and the volumetric pump [6,7]. The saline leaves the joint either through leakage along an access portal or through a separate outflow cannula (Fig. 1).

Previously, guidelines were presented to improve irrigation using steady state conditions [4]. However, these are insufficient for developing new techniques to achieve optimal joint irrigation. To study the complex clinical practice of irrigation, a physical simulation environment was developed that incorporates the main characteristics for performing arthroscopy. The concept consists of (a) maintaining the normal operating setting, (b) replacing the human joint by a phantom, and (c) incorporating registration devices, i.e., camera, pressure, and flow sensors. The operating setting includes the following equipment: arthroscope, light source, camera, pump, tubing, instruments, sheaths, and cannulae (Fig. 1(*a*)).

A physical phantom was preferred over the use of human cadaver material and virtual reality systems [8–10] for the following reasons. The physical phantom would

- exclude any time constraints and complications (opposed to cadaveric material)
- enable the study of parameters in a controlled setting (opposed to cadaveric material)
- have a good resemblance with reality (opposed to virtual reality systems)
- enable repeated surgical actions in a natural fashion such as irrigation, inspection, cutting of tissue, and manipulation of the joint (opposed to virtual reality systems)
- facilitate the measurement of characteristics such as pressure, flow, and flow patterns (opposed to cadaveric material and virtual reality systems)

The human knee joint was chosen for modeling because knee arthroscopies are most frequently performed [11], and some results can presumably be generalized to other joints.

The goal of this paper is to present the development of the knee phantom with integrated registration devices specifically apt for studying joint irrigation. Subsequently, experimental validation is presented of the knee phantom's characteristics.

2 Design

2.1 Requirements for the Knee Phantom. Neither in literature [3,12,13] nor on the market [14,15] are physical phantoms

Manuscript received July 9, 2008; final manuscript received March 5, 2009; published online May 27, 2009. Review conducted by Jaydev Desai. Paper presented at the Design of Medical Devices Conference, Minneapolis, MN, April 17–19 2007. Poster Presentation.

 Copyright © 2009 by ASME

Downloaded 28 May 2009 to 131.180.28.156. Redistribution subject to ASME license or copyright; see http://www.asme.org/terms/Terms_Use.cfm

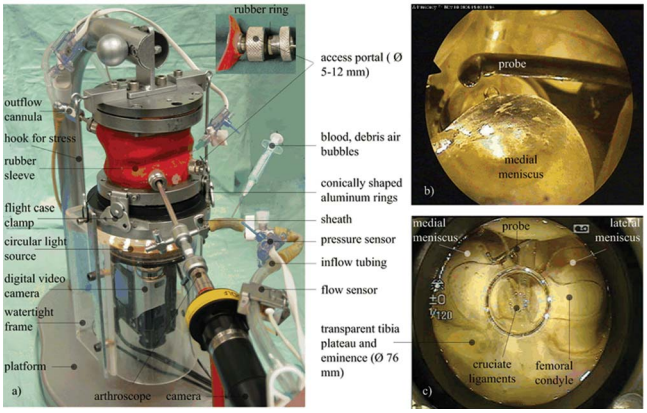

Fig. 1 (*a*) Prototype of the knee phantom, (*b*) arthroscopic view showing a probe (routinely used instrument to inspect the joints arthroscopically), and (*c*) overview from underneath the transparent tibial surface showing the location of the probe in the knee phantom.

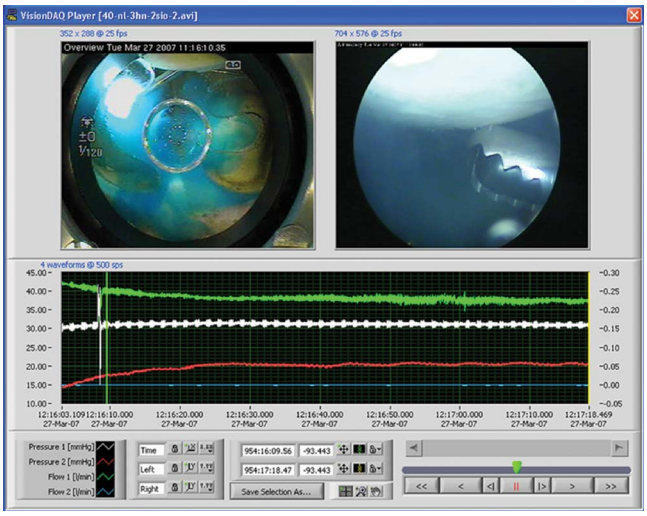

Fig. 2 Interface of the VISIONDAQ player showing two recorded images and four data signals. Left: The view form underneath the tibial surface. Right: The arthroscopic view. Bottom: Four colored data signals; the upper and lower signal indicate the flow, and the two signals in the middle indicate the pressure. The two digital video streams and the four data signals can be saved separately for further processing. Additional functions enable scrolling and zooming on the recorded signals.

available that have both an anatomical appearance and allow for realistic irrigation and surgical actions. Consequently, we aimed at the development of a knee phantom that would incorporate both. The three main requirements were as follows.

1. *Anatomic appearance.* From analysis of 30 arthroscopic knee operations and prior experience with a simplified knee phantom [13], the following anatomic structures had to be present: the femoral and tibial condyles, the tibial eminence, the menisci, and the cruciate ligaments. The surrounding capsule was considered as one structure. The anatomic structures should match human shape and geometry and allow the development of natural flow patterns [16].
2. *Required surgical items*. Three most commonly used access portals had to be included. These were the anterolateral, the anteromedial, and the superomedial portals [17,18]. Analogous to the clinical practice, the portals should allow for some leakage. To facilitate a simple surgical operation, the menisci had to be cut and afterward replaced by new pairs to start a new operative session. Lastly, stressing of the knee phantom should be allowed to increase operative joint space in the medial or lateral knee compartment.
3. *Ability to study irrigation.* The hydrostatic and hydrodynamic behavior during irrigation should match that of human knee joints, and simulation of disturbances of the arthroscopic view should be possible such as blood, debris, and air bubbles. Besides mimicking the correct behavior, measurement of the pressure and flow is required, as well as the visualization and registration of flow patterns in the knee phantom.

2.2 Prototype. A knee phantom was designed on the basis of the requirements (Fig. 1). The femoral condyles are adapted from an anatomical model (SOMSO, Breukhoven, The Netherlands (NL)). The tibial surface is made of 2 mm thick glass since glass enables an undisturbed view of the complete interior of the knee phantom. Additionally, glass is relatively insensitive to scratches. The tibial eminence has a semispherical shape of 28 mm as a compromise between distortion of the transparent view and its resemblance with true anatomy. The femoral condyles were placed at a 90 deg angle relative to the tibial surface.

This way the natural starting position is simulated for performing a knee arthroscopy with an upper leg positioned horizontally on the operating table and a lower leg hanging at 90 deg from the operating table.

The menisci are cast of transparent silicone rubber (PS 61, Poly-Service, The Netherlands). The cruciate ligaments consist of transparent silicone tubing. Underneath the tibial surface, a specially designed watertight frame was placed that houses a digital video camera (JVC GR D93, JVC, The Netherlands), and a custom-made light source consisting of a ring with 12 uniformly distributed light-emitting diodes (LEDs, 5 mm Warm Weiss 20 deg, Stuut en Bree, The Netherlands) connected to a standard 12 V adapter. To prevent reflection and to ensure uniform illumination of the entire knee phantom, the LEDs were placed in the horizontal plane, 56 mm from the center and 50 mm below the tibial plane with an orientation of 50 deg from the horizontal. This facilitates postprocessing of video recordings. Documentation of flow patterns is achieved by visualizing them with colored ink (e.g., blue) and video recording (Fig. 2) [13].

A sleeve of natural rubber (thickness is 1 mm and outer diameter is 85 mm, Schiema Rubber & Kunststoffen BV, The Netherlands) was chosen to materialize the surrounding capsule. The sleeve is clamped between two pairs of custom-made conically shaped aluminum rings. The knee phantom was partly filled up with soft silicone (Smooth-Sil 910, AFF Materialen, The Netherlands) to reduce the volume to around 95 ml and to reshape its interior more anatomically. The menisci can be substituted as the flight case clamps give easy access to the joint (Fig. 1(*a*)). The three portals are placed in the rubber sleeve according to directions from literature [17,18]. They allow leakage, if required, by replacing rubber rings in the stainless steel housing by ones with differently sized holes (Fig. 1(*a*): upper part).

Natural stressing of the knee joint is a combination of internal/external rotation and varus/valgus positioning, but in the knee phantom the artificial cruciate ligaments cannot be loaded. As a result, stressing in predominantly varus or valgus direction gave a similar arthroscopic view where separation of the tibial surface from the femoral condyles is seen. Stressing is performed by manually applying load to the upper and lower aluminum rings. This load can be maintained using the hooks on both sides of the rubber sleeve (Fig. 1(*a*)). Finally, the knee phantom is hung in an arm, which is connected to a platform. On the platform, a reservoir can be placed to collect fluid from portal leakage.

2.3 Registration Devices. A data acquisition system (VISIONDAQ, Version 1.2) was developed that enables the synchronized acquisition of four data channels and two digital video streams,

Downloaded 28 May 2009 to 131.180.28.156. Redistribution subject to ASME license or copyright; see http://www.asme.org/terms/Terms_Use.cfm

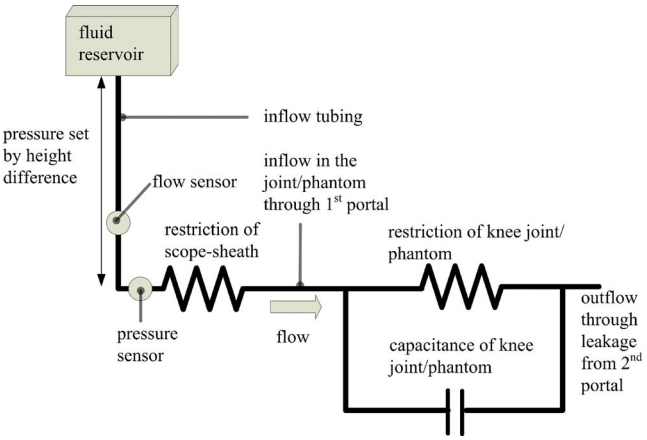

Fig. 3 Schematic drawing of the irrigation setting in the operating room and simulation environment. The sheath is modeled as a restriction, and the knee joint or phantom as a restriction placed in a parallel circuit with a capacitance. In inflow tubing has negligible characteristics. The pressure and flow were measured at the indicated locations both in the operating room and the simulation environment.

i.e., the view from underneath the tibial surface and the arthroscopic view (Figs. 1 and 2). The advantage of the video recording underneath the tibial surface is that phenomena occurring in the entire joint can be documented. The data channels were assigned to two pressure sensors (Baxter T 310196 A, Edwards Life Sciences, The Netherlands) and two flow sensors (7C flow probe, Transonic Systems, The Netherlands) that can be placed in different locations in the irrigation system. The sample rate of the data channels was set at 500 Hz, but can be changed accordingly. The hardware and software (LABVIEW 7.0, National Instruments) allow for expansion to acquire additional data signals. Acquisition was performed with a consumer notebook (HP Compaq NC6120 P-M 750, Megasellers, The Netherlands). The video streams were preprocessed with a video server (Axis 241Q, Axis Communications AB, Sweden), and the data signals were amplified and digitized (PMD 1208FS, Measurement Computing). All data can be analyzed with a special viewer and saved for further processing in standard digital video and data formats (Fig. 2). These registration devices were used both for measurements in the simulation environment and the operating room.

3 Validation

Validation of the knee phantom for studying joint irrigation was based on its functional appearance, and hydrostatic and hydrodynamic behavior. For the latter two items, data were compared that were measured during normal knee arthroscopies in patients. The options were limited for measuring pressure and flow in the operating room. Therefore, the irrigation process was described with a model that facilitated the selection of comparable data (Fig. 3).

3.1 Functional Appearance. Evaluation of functional appearance implies the verification of the interior anatomic structures of the knee phantom and the ability to perform ordinary surgical actions. Therefore, four orthopedic surgeons (more than 50 arthroscopies a year) and four residents (less than 50 arthroscopies performed) were invited to perform actions including inspection with a probe, cutting of meniscal tissue, and irrigation. Subsequently, they were given a short questionnaire on their impressions. The proper shape and spacing of the main anatomic structures are not only relevant for surgical items but also for stimulation of natural flow patterns in the knee phantom. The overall flow patterns cannot be documented in human knee joints. However, it is assumed that the main anatomic structures and the location of the portals determine to a large extent the course of flow patterns [13]. Sufficient anatomic imitation and simulation of disturbances were verified by questioning the surgeons.

3.2 Modeling Irrigation Process. The operative irrigation setup that is normally used in the day care center of the Academic Medical Centre consisted of a gravity pump (routinely set operating pressure was 6.5 kN/m^2 (equal to 49 mm Hg) and a two-portal technique. Inflow takes place through the arthroscope-sheath combination in one portal, e.g., the left anteromedial portal (Fig. 1(*a*)) where the arthroscope is inserted. Outflow takes place predominantly through leakage from the second portal, which is used for instruments, e.g., the right anterolateral portal (Fig. 1(*a*)). No third superomedial portal is made for the two-portal technique. This operative setup could be copied exactly in the simulation environment with the difference that the human knee joint was replaced by the knee phantom. From a systems control perspective, this configuration is an open loop system. In steady state, the flow is constant throughout the entire system, and the pressure drops proportionally with the restriction of subsystems to the atmospheric pressure level that was set at 0 bar (Fig. 3) [4].

Ideally, only the restriction of human knee joints has to be determined and compared with the restriction of the knee phantom to validate the hydrostatic behavior. However, in the operating room it was difficult to measure the intra-articular pressure. Instead, the pressure drop along the combined restriction of the sheath and the knee joints or phantom was used. This choice is justified because the same equipment was used in both the operating room and the simulation environment, and the pressure and flow were measured at exactly the same locations (Fig. 3). Theoretically, the knee phantom's restriction is solely dependent on the size of the cross-sectional area of the outflow portal, assuming that no leakage takes place elsewhere in the system. With this, it was stated that the restriction of the knee phantom would be validated if the measured range of combined restrictions of the sheath and the human knee joints could be imitated in the simulation environment. The imitation would be achieved by proper selection of the size of the outflow portal.

Besides this hydrostatic characteristic, we were interested in the hydrodynamic behavior. Only the elasticity of the surrounding capsule and ligaments contributed to this behavior. Thereto, the human knee joints and the knee phantom were additionally modeled with a capacitance placed in a parallel circuit with the restriction (Fig. 3). Ideally, the dynamic behavior of the knee joints and phantom would be determined by producing a step in the pressure signal and measuring the flow response inside the knee.

Exciting a proper step signal was not feasible in the operating room. Instead, two other comparisons were performed. First, an average capacitance of human knee joints was determined from a nonlinear pressure-volume relation of human knee joints available in literature [19]. Thereto, this relation was mirrored to achieve the volume-pressure relation and linearized at the normal operating pressure (6.5 kN/m^2). The slope of the linearized volume-pressure curve was assumed to be a reasonable value for the capacitance. For the knee phantom, the linear volume-pressure curve is determined by the elasticity of the surrounding sleeve. With this, it was stated that the capacitance of the knee phantom would be validated if the slope of the volume-pressure curve of the sleeve(s) could be tuned such that its value would have the same order of magnitude as the capacitance derived from literature.

Second, stressing of the knee joint to create workspace was used for hydrodynamic evaluation. This frequently occurring action gave a dynamic response in the pressure and flow and could be imitated in the simulation environment. The stressing forces were not measured in both setups; only the changes in pressure and flow as a result of the stressing were registered. The hydrodynamic behavior was evaluated with Fourier spectra where the measured pressure was chosen as input signal and the measured flow as output signal. As both settings were identical, except for the knee, and the irrigation process was an open loop system (Fig. 3), it was assumed that the hydrodynamic behavior would be vali-

Downloaded 28 May 2009 to 131.180.28.156. Redistribution subject to ASME license or copyright; see http://www.asme.org/terms/Terms_Use.cfm

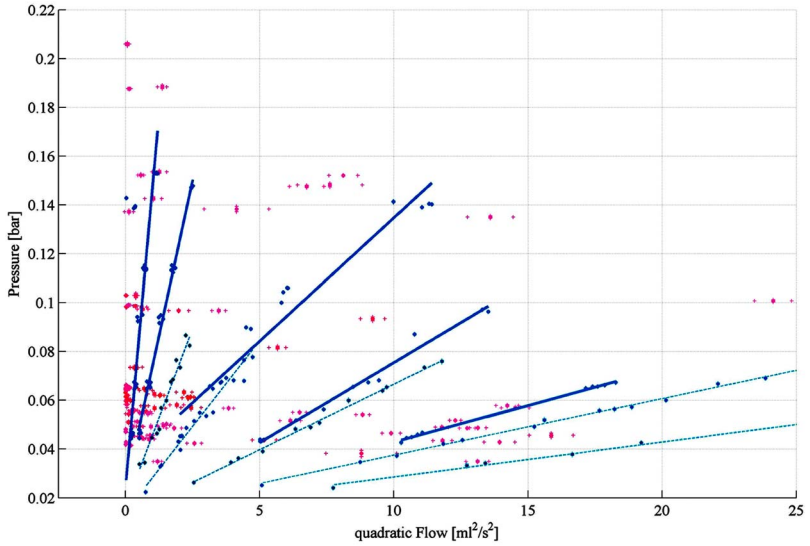

Fig. 4 The solid circles represent the mean pressure and flow as measured at the locations shown in Fig. 3. The plus signs indicate the standard deviations. The light colored circles indicate data of the 17 patients and the dark circles those of 10 conditions of the knee phantom. The lines are the regression lines for each condition. Their slopes determine the value of the combined restriction of the sheath and knee phantom. The steepest line is the condition with a triple stack of rubber rings of Ø1 mm and the initial phantom volume of 95 ml, and the flattest line is the condition with a single rubber ring of Ø3 mm and a volume of 80 ml.

dated if the range of dynamic changes measured in the operating room could be imitated in the simulation environment.

3.3 Measurements and Comparison. The arthroscopic view and the view on the hand of the surgeon, pressures, and flows (see Fig. 3 for measurement locations) were acquired during normal arthroscopic knee operations of 17 patients using the VISIONDAQ hardware and software. The operation time was 28 min on average (standard deviation of 14 min). The patient population consisted of eight males and nine females; eight were operated on the left knee and nine on the right knee by five different surgeons. 12 of the 17 operations were meniscectomies, 4 were nettoyages, and 1 was a diagnostic arthroscopy. The measurement protocol was approved by the Medical Ethical Committee. All patients signed an informed consent to accept the registration of their procedure.

For validation of the combined restriction of sheath and knee phantom, pressure and flow measurements from the operating room were selected at steady state conditions and without an instrument inserted in the second portal. The presence of an instrument was verified from the recorded arthroscopic view. The restrictions were expressed as the quotient of the pressure and the squared flow (10^{17} N $s^2/m^8 = 1$ bar s^2/ml^2) because it was most likely that a turbulent flow would exist [20]. The pressure and flow were measured under the same conditions in the simulation environment using the VISIONDAQ hardware and software. Thereto, the superomedial portal was closed, and leakage was prevented along the anteromedial portal in which the arthroscope was placed. The fluid restriction of the knee phantom was varied by changing the diameter of the holes of the rubber rings in the anterolateral portal (Fig. 1(*a*): upper part). The holes ranged from a stack of three rubber rings (∅1 mm) at overlapping locations to one rubber ring with a diameter of ∅3 mm. Additionally, the restriction was influenced by using two different initial volumes of the knee phantom (95 ml and 80 ml), which was achieved by stressing.

The capacitance of the knee phantom (10^{-11} $m^5/N = 1$ ml/bar) was determined by a quasistatic increase in the pressure (from 0 bar to 0.1 bar) and measuring the volume change using the VISIONDAQ hardware and software. Measurements were done with one and two layers of the rubber sleeve (Fig. 1(*a*)). From these measurements, a linear fit was determined and its derivative was the capacitance for comparison.

For the assessment of the hydrodynamic behavior, the presence of joint stressing without an instrument in the portal was verified from both video streams. A total of 76 sections (in 16 patients) could be selected. To determine the Fourier spectra, the pressure and flow signals were removed of their means, filtered, and resampled to 25 Hz with standard MATLAB routines (MATLAB, Version 7.0.4.365 (R14), The Mathworks, Natick, NA). The mean Fourier spectrum of 16 knee joints was determined as well as the upper and lower boundary spectra. In the knee phantom, stressing was performed by a manually applied load on the upper and lower aluminum rings at the medial or lateral side of the knee phantom. Loading was increased until the femoral condyle touched the glass tibial surface. The stress was applied quickly, maintained for around 5 s, released quickly, and left at its original position for 5 s. This cycle was repeated at least six times for each of the four different cross-sectional areas of the anterolateral outflow portal: single, double, and triple stacks of rubber rings of ∅1 mm, and a single rubber ring of ∅2 mm (Figs. 1 and 5).

4 Results

All eight participants agreed that the sizing and shape of anatomic structures were sufficiently imitated, especially if viewed through the arthroscope. The portals were correctly positioned, and the insertion of the instruments felt natural. Furthermore, basic surgical actions could be performed by all participants in the knee phantom. Five participants indicated that the joint space was sufficient, whereas the others found it a bit too large. The residents were initially troubled by the mirroring of the transparent menisci in the tibial surface. All participants agreed that the disturbances (bleeding, air bubbles, and loose fibrous tissue) were realistically imitated.

A wide range of pressure and flow combinations were measured during the arthroscopic surgeries of the 17 patients (Fig. 4). The

Downloaded 28 May 2009 to 131.180.28.156. Redistribution subject to ASME license or copyright; see http://www.asme.org/terms/Terms_Use.cfm

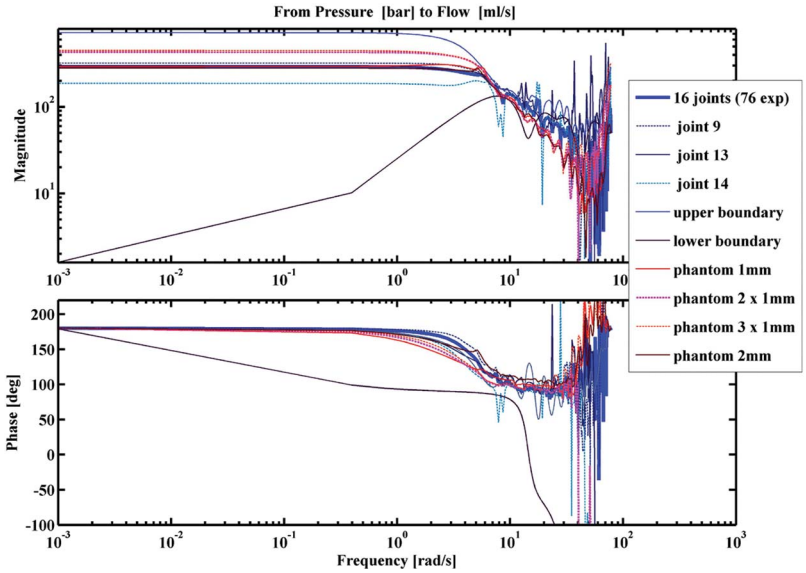

Fig. 5 Fourier spectra of stressing performed on human knee joints (see legend) and the knee phantom (see legend). The mean and upper and lower boundary Fourier spectra of 16 knee joints are drawn. Hydrodynamic changes due to stressing of the knee phantom were determined for four different cross-sectional areas of the anterolateral portal: single (phantom 1 mm), double (phantom 2×1 mm), triple (phantom 3×1 mm) stacks of rubber rings of Ø1 mm, and a single rubber ring of Ø2 mm (phantom 2 mm).

median combined restriction of the sheath, and the 17 human knee joints were determined at 0.718×10^{18} N s^2/m^8 with a minimum of 0.0266×10^{18} N s^2/m^8 and a maximum of 29.3×10^{18} N s^2/m^8. The regression lines are shown for ten different conditions measured in the knee phantom (Fig. 4). Their slopes represent the range of combined restrictions of the sheath and the knee phantom that could be reached. The smallest value of 0.0143×10^{18} N s^2/m^8 was reached for the condition with a single rubber ring of ∅3 mm and an initial phantom volume of 80 ml. The largest value of 1.22×10^{18} N s^2/m^8 was determined for the condition with a triple stack of rubber rings of ∅1 mm and the initial phantom volume of 95 ml.

The derivative of the volume-pressure relation at 6.5 kN/m^2, representing the capacitance of human knee joints, was determined to be 6.89×10^{-9} m^5/N and that of the knee phantom was calculated to be 7.50×10^{-9} m^5/N. To achieve this, a double layer of the rubber sleeve had to be used.

The mean and lower and upper boundaries of the Fourier spectra are shown when stressing the 16 human knee joints as well as those of three representative human knee joints (Fig. 5). For these three (joints 9, 13, and 14), the Fourier spectra were shown separately because we were able to collect at least nine samples with relatively low noise for these knee joints. Additionally, they show different static magnitudes, which indicate the variability in human knee joint behavior. Hydrodynamic changes due to stressing of the knee phantom were determined for four different cross-sectional areas of the anterolateral portal (Fig. 5). A positive phase of 180 deg is present, because the fluid in the joint or phantom is pushed out, thereby changing the direction of the flow sensor measurement in the inflow tubing.

5 Discussion and Conclusion

A physical simulation environment for studying arthroscopic joint irrigation was developed. Specific design choices were made for the knee phantom to represent human knee joints: key anatomic structures of human proportions. On the other hand, specific design choices counter to actual human joints were made to enable better irrigation study: transparency of the tibial surface, menisci and cruciate ligaments, and the ability to measure pressure, flow, and flow patterns. In general, surgeons agreed that the knee phantom sufficiently imitated human knee joints to perform routine surgical treatment actions: joint inspection, meniscectomy, and removal of corpus libera. Especially, the inherently present force feedback and the arthroscopic view on the anatomic structures with the possibility of simulating disturbances were highly appreciated. On the other hand, stressing of the joint requires a more natural setup with a lower leg, and the transparent structures can be confusing at times. Performing more complex arthroscopic surgeries is not possible with the current knee phantom.

By modeling the operation setting from a systems control approach, we were able to simplify the complex clinical practice and capture the knee phantom's hydrostatic and hydrodynamic behavior with a fairly small set of experiments. The high value of the maximum combined restriction determined in the operating room could be caused by obstruction of leakage along the portal, or fluid extravasation into the body instead of leakage along the portal (Fig. 4). As the magnitude of the spectra also represents the combined restriction, the upper boundary can be explained analogously (Fig. 5). The presence of the lower boundary of the human joints could be attributed to a temporary increase in the outflow portal due to stretching of the tissue around the incision when stressing the knee joint. Stressing of the joint was not carefully orchestrated in the operating room. In a future experiment, the quality of the data could be improved by standardization of stressing during a part of the operation. On the other hand, even for the current data, the Fourier spectra are acceptably similar for the human knee joints and the knee phantom (Fig. 5).

The results indicate a substantial variation in human knee joints. Since we were able to tune the restriction, the starting volume, and the capacitance of the knee phantom in an easy fashion, we could virtually match the irrigation behavior of each individual human knee joint with the precondition that pressure and flow measurements of that particular human knee joint would be available. Only if hydrodynamic behavior has to be investigated at higher set pressure levels (>80 mm Hg), probably a third rubber sleeve needs to be added in the knee phantom to increase its

Downloaded 28 May 2009 to 131.180.28.156. Redistribution subject to ASME license or copyright; see http://www.asme.org/terms/Terms_Use.cfm

capacitance. This requires constructive adjustment of the aluminum rings. Overall, the results justify validation as the tunable range of predominant parameters of the knee phantom is substantial and realistic. Future studies could include analysis of local pressures or flow pattern changes due to instrument motions or removal of anatomic structures. This merely requires the addition of a (small) pressure sensor inside the knee phantom.

As we present a prototype, some adjustments are required for future intensive use of the simulation environment. Some parts are fragile (menisci) or show changes in material properties over time (rubber sleeve). These have to be replaced by other materials. Additionally, stressing of the knee phantom has to be redesigned to perform natural joint stressing by pushing against a dummy lower leg.

In conclusion, the interior of the knee phantom is not only shaped sufficiently anatomical but it behaves hydrostatically and hydrodynamically within the existing intersubject variation in human knee joints where it concerns joint irrigation. Thus, a platform for in vitro simulation was realized that mimics real-life situations with challenged view. Besides the evident use for studying irrigation phenomena, the physical simulation environment is sufficiently realistic to be used for evaluation of other (new) surgical instruments, and forms a basis to evolve as a training environment to learn arthroscopic skills before starting in the operating room.

Acknowledgment

This work was supported by the Technology Foundation STW, Applied Science Division of NWO, and the Technology Program of the Ministry of Economic Affairs, The Netherlands. Richard Wolf Endoscopy Belgium, Gent, Belgium provided all arthroscopic equipment. The authors wish to thank P. Broekhuijsen and R. Tigchelaar (Department of MTO, Academic Medical Centre (AMC), Amsterdam, The Netherlands) and W. Hofland and M. van Nieuwenhuizen for their valuable contributions in the construction of the knee phantom. Furthermore, they appreciate the help of I. Sierevelt (Department of Orthopaedic Surgery, AMC, Amsterdam, The Netherlands) for statistics and A. Schouten (Delft University of Technology, Delft, The Netherlands) for system identification.

References

[1] Morgan, C. D., 1987, "Fluid Delivery Systems for Arthroscopy," Arthroscopy: J. Relat. Surg., **3**(4), pp. 288–291.
[2] Ogilvie-Harris, D. J., and Weisleder, L., 1995, "Fluid Pump Systems for Arthroscopy: A Comparison of Pressure Control Versus Pressure and Flow Control," Arthroscopy: J. Relat. Surg., **11**(5), pp. 591–595.
[3] Muellner, T., Menth-Chiari, W. A., Reihsner, R., Eberhardsteiner, J., and Engebretsen, L., 2001, "Accuracy of Pressure and Flow Capacities of Four Arthroscopic Fluid Management Systems," Arthroscopy: J. Relat. Surg., **17**(7), pp. 760–764.
[4] Tuijthof, G. J., Dusee, L., Herder, J. L., van Dijk, C. N., and Pistecky, P. V., 2005, "Behavior of Arthroscopic Irrigation Systems," Knee Surg. Sports Traumatol. Arthrosc, **13**(3), pp. 238–246.
[5] Tuijthof, G. J., Sierevelt, I. N., and van Dijk, C. N., 2007, "Disturbances in the Arthroscopic View Defined With Video Analysis," Knee Surg. Sports Traumatol. Arthrosc, **15**(9), pp. 1101–1106.
[6] Tuijthof, G. J. M., van den Boomen, H., van Heerwaarden, R. J., and van Dijk, C. N., 2008, "Comparison of Two Arthroscopic Pump Systems Based on Image Quality," Knee Surg. Sports Traumatol. Arthrosc, **16**(6), pp. 590–594.
[7] Ampat, G., Bruguera, J., and Copeland, S. A., 1997, "Aquaflo Pump vs FMS 4 Pump for Shoulder Arthroscopic Surgery," Ann. R. Coll. Surg. Engl., **79**, pp. 341–344.
[8] Mabrey, J. D., Cannon, W. D., Gillogly, S. D., Kasser, J. R., Sweeney, H. J., Zarins, B., Mevis, H., Garrett, W. E., and Poss, R., 2000, "Development of a Virtual Reality Arthroscopic Knee Simulator," Stud. Health Technol. Inform., **70**, pp. 192–194.
[9] Pedowitz, R. A., Esch, J., and Snyder, S., 2002, "Evaluation of a Virtual Reality Simulator for Arthroscopy Skills Development," Arthroscopy: J. Relat. Surg., **18**(6), p. E29.
[10] Riener, R., Frey, M., Proll, T., Regenfelder, F., and Burgkart, R., 2004, "Phantom-Based Multimodal Interactions for Medical Education and Training: The Munich Knee Joint Simulator," IEEE Trans. Inf. Technol. Biomed., **8**(2), pp. 208–216.
[11] van Dijk, C. N., 2002, *Beweegredenen, de patient als bron van inspiratie*, Inaugural University of Amsterdam, Amsterdam, The Netherlands.
[12] Dolk, T., and Augustini, B. G., 1989, "Three Irrigation Systems for Motorized Arthroscopic Surgery: A Comparative Experimental and Clinical Study," Arthroscopy: J. Relat. Surg., **5**(4), pp. 307–314.
[13] Tuijthof, G. J., Herder, J. L., and van Dijk, C. N., 2008, "Experimental Approach to Study Arthroscopic Irrigation," Med. Eng. Phys., **30**(8), pp. 1071–1078.
[14] Pacific Research Laboratories, Inc., "Sawbones," http://www.sawbones.com/.
[15] Hillway Surgical Ltd., "Advanced Models for Simulated Surgery," http://www.surgimodels.com/default.htm.
[16] Tatari, H., Dervisbey, M., Muratli, K., and Ergor, A., 2005, "Report of Experience in 190 Patients With the Use of Closed Suction Drainage in Arthroscopic Knee Procedures," Knee Surg. Sports Traumatol. Arthrosc, **13**(6), pp. 458–462.
[17] Sisk, T. D., 1987, "Arthroscopy of Knee and Ankle," *Campbell's Operative Orthopedics*, A. H. Crenshaw, ed., Mosby, St. Louis, MO, pp. 2547–2608.
[18] Brophy, R., Dunn, W., and Wickiewicz, T., 2004, "Arthroscopic Portal Placement," Tech. Knee Surg., **3**(1), pp. 2–7.
[19] Oretorp, N., and Elmersson, S., 1986, "Arthroscopy and Irrigation Control," Arthroscopy: J. Relat. Surg., **2**(1), pp. 46–50.
[20] Leijdens, H., 1992, *Stroming en warmteoverdracht I*, DUT, Delft, The Netherlands, in Dutch.

Downloaded 28 May 2009 to 131.180.28.156. Redistribution subject to ASME license or copyright; see http://www.asme.org/terms/Terms_Use.cfm